

## Physics Input from Multiwavelength Observations of AGN

M. Böttcher<sup>1</sup>

*Physics and Astronomy Department, Rice University, MS 108, Houston, TX 77005-1892, USA*

**Abstract.** The current status of leptonic jet models for blazars is reviewed. Differences between the quasar and BL-Lac subclasses of blazars may be understood in terms of the dominance of different radiation mechanisms in the gamma-ray regime. Spectral variability patterns of different blazar subclasses appear to be significantly different and require different intrinsic mechanisms causing gamma-ray flares. As examples, recent results of long-term multiwavelength monitoring of PKS 0528+134, 3C 279, and Mrk 501 are interpreted in the framework of leptonic jet models. Short-term variability patterns give important additional clues about the source geometry and the relevant radiation mechanisms in blazars. Challenges for future observational efforts are discussed.

*Key words:* Active galaxies, extragalactic jets, theory, radiation mechanisms

### 1. Introduction

Recent high-energy detections and simultaneous broadband observations of blazars, determining their spectra and spectral variability, are posing strong constraints on models of blazars. 66 blazars have been detected by EGRET at energies above 100 MeV (Hartman et al. 1999), the two nearby high-frequency peaked BL Lac objects (HBLs) Mrk 421 and Mrk 501 are now multiply confirmed sources of multi-GeV – TeV radiation (Punch et al. 1992, Petry et al. 1996, Quinn et al. 1996, Bradbury et al. 1997), and the TeV detections of PKS 2155-314 (Chadwick et al. 1999) and 1ES 2344+514 (Catanese et al. 1998) are awaiting confirmation. Most EGRET-detected blazars exhibit rapid variability (e.g., Mukherjee et al. 1997), in some cases on intraday and even sub-hour (e. g., Gaidos et al. 1996) timescales, where generally the most rapid variations are observed at the highest photon frequencies.

---

<sup>1</sup> Chandra Fellow

The broadband spectra of blazars consist of at least two clearly distinct spectral components (e.g., von Montigny et al. 1995). The first one extends in the case of flat-spectrum radio quasars (FSRQs) from radio to optical/UV frequencies, in the case of HBLs up to soft and even hard X-rays, and is consistent with non-thermal synchrotron radiation from ultrarelativistic electrons. The second spectral component emerges at  $\gamma$ -ray energies and peaks at several MeV – a few GeV in most quasars, while in the case of some HBLs the peak of this component appears to be located at TeV energies.

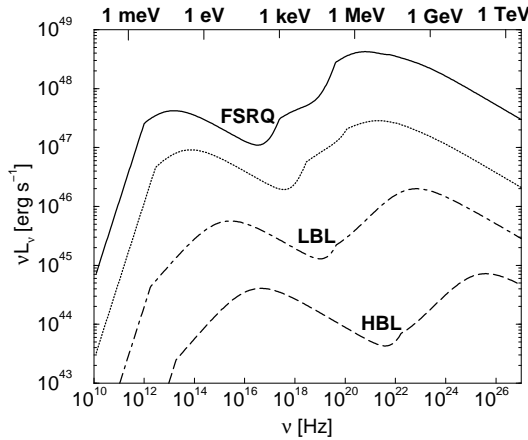


**Figure 1.** Schematic, prototypical broadband spectra of different blazar classes.

The different sub-classes of blazars exhibit markedly different spectral variability patterns. In quasars, the relative amplitude of a  $\gamma$ -ray flare,  $\delta L_{\text{HE}}$ , is generally larger than the corresponding variability amplitude at lower energies (i.e. in the synchrotron component),  $\delta L_{\text{LE}}$ , and the  $\gamma$ -ray dominance during flares may be super-quadratic, i.e.  $\delta L_{\text{HE}} \sim \delta L_{\text{LE}}^\alpha$  with  $\alpha \geq 2$  (e.g., Wehrle et al. 1998). The  $\gamma$ -ray spectra generally harden during  $\gamma$ -ray flares, although the  $\nu F_\nu$  peak of either of the spectral components has so far not been seen to shift in any systematic way (see, however, Böttcher [1999] for a prediction on the expected synchrotron peak shift). Detailed short-term variability studies show generally no consistent patterns of timelags between different energy bands (e.g., Hartman et al. 2001b).

Spectral variability of high-frequency peaked BL Lac objects is also generally characterized by a higher variability amplitude in  $\gamma$ -rays than at lower frequencies, but here we generally find a sub-quadratic amplitude behavior, i. e.  $\delta L_{\text{HE}} \sim \delta L_{\text{LE}}^\alpha$  with  $\alpha \leq 2$  (e.g., Petry et al. 2000). HBL flares are accompanied by spectral hardening in both components, and the synchrotron peak shifts significantly to higher frequency during flares (e.g., Takahashi et al. 1996, Pian et al. 1998, Urry et al. 1997). Within the synchrotron emission component, there is a consistent time-lag trend with flares at higher frequencies systematically preceding lower-frequency flares by an amount consistent with being due to synchrotron cooling (e.g., Takahashi et al. 1996, Edelson et al. 1995). More detailed analyses of time-resolved HBL spectra during flaring activity often show a clockwise rotation when plotted in a hardness-intensity diagram (e.g., Takahashi et al. 1996).

The bolometric luminosity of EGRET-detected quasars and some low-frequency peaked BL Lac objects (LBLs) during flares is dominated by the  $\gamma$ -ray emission. If this emission were isotropic, it would correspond to enormous luminosities (up to  $\sim 10^{49}$  erg s $^{-1}$ ) which, in combination with the short observed timescales (implying a small size of the emission region) would lead to a strong modification of the emissivity spectra by  $\gamma\gamma$  absorption, in contradiction to the observed smooth power-laws at EGRET energies. This has motivated the concept of relativistic beaming of radiation emitted by ultrarelativistic particles moving at relativistic bulk speed along a jet (for a review of these arguments, see Schlickeiser 1996). While it is generally accepted that blazar emission originates in relativistic jets, the radiation mechanisms responsible for the observed  $\gamma$  radiation are still under debate. It is not clear yet whether in these jets protons are the primarily accelerated particles, which then produce the  $\gamma$  radiation via photo-pair and photo-pion production, followed by  $\pi^0$  decay and synchrotron emission by secondary particles (e. g., Mannheim 1993) or by the primarily accelerated protons themselves (Aharonian 2000, Mücke & Protheroe 2000), or electrons (and positrons) are accelerated directly and produce  $\gamma$ -rays in Compton scattering interactions with the various target photon fields in the jet (Marscher & Gear 1985, Maraschi et al. 1992, Dermer et al. 1992, Sikora et al. 1994, Ghisellini & Madau 1996, Böttcher et al. 1997, Blażejowski et al. 2000).

In this review, I will describe the current status of blazar models based on leptons as the primary constituents of the jet which are responsible for the  $\gamma$ -ray emission. For a recent review of hadronic jet models see, e.g., Rachen (1999). In Section 2, I will give a description of the common features present in the different variations of these models and discuss the different  $\gamma$ -ray production mechanisms and their relevance for different blazar classes. In Section 3, I will review recent progress in understanding intrinsic differences between different blazar classes. In Section 4, I will discuss broadband spectral variability of individual blazars and their interpretation in the framework of leptonic jet models. Finally, in Section 5, I will discuss some open questions with respect to our understanding of blazar spectra and variability, and challenges for future observations to address some of these questions.

## **2. Salient features of leptonic jet models**

The basic geometry of leptonic blazar jet models is illustrated in Fig. 2. At the center of the AGN, an accretion disk around a supermassive, probably rotating, black hole is powering a relativistic jet. Along this pre-existing jet structure, occasionally blobs of ultrarelativistic electrons are ejected at relativistic bulk velocity.

The electrons are emitting synchrotron radiation, which will be observable at IR – UV or even X-ray frequencies, and hard X-rays and  $\gamma$ -rays via Compton scattering processes. Possible target photon fields for Compton scattering are the synchrotron photons produced within the jet (the SSC process, Marscher & Gear 1985, Maraschi et al. 1992, Bloom & Marscher 1996, Georganopoulos & Marscher 1998b), the UV – soft X-ray emission from the disk — either entering the jet directly (the ECD [External Comptonization of Direct disk radiation] process; Dermer et al. 1992, Dermer & Schlickeiser 1993) or after reprocessing at the broad line regions or other circumnuclear material (the ECC

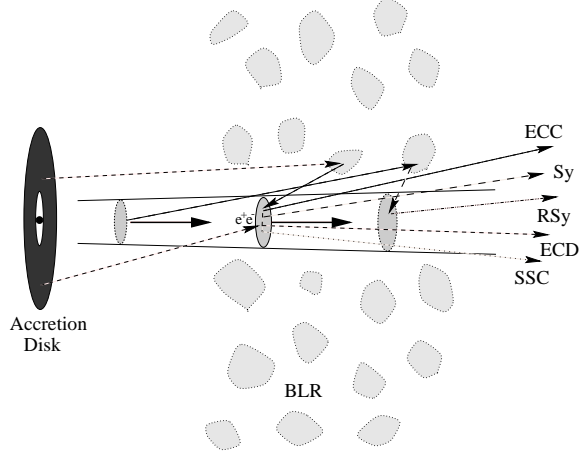


**Figure 2.** Illustration of the model geometry and the relevant  $\gamma$  radiation mechanisms for leptonic jet models.

[External Comptonization of radiation from Clouds] process; Sikora et al. 1994, Blandford & Levinson 1995, Dermer et al. 1997), or jet synchrotron radiation reflected at the broad line regions (the RSy [Reflected Synchrotron] mechanism; Ghisellini & Madau 1996, Bednarek 1998, Böttcher & Dermer 1998). It has recently also been suggested that infrared emission from circumnuclear dust may play a significant role as seed photon field for Compton scattering in the jet (Blažejowski et al. 2000, Abeiter et al. 2001).

The relative importance of these components may be estimated by comparing the energy densities of the respective target photon fields. Denoting by  $u'_B$  the co-moving energy density of the magnetic field, the energy density of the synchrotron radiation field, governing the luminosity of the SSC component, may be estimated by  $u'_{sy} \approx u'_B \tau_T \gamma_e^2$ , where  $\tau_T = n'_{e,B} R'_B \sigma_T$  is the Thomson depth of the relativistic plasma blob and  $\gamma_e$  is the average Lorentz factor of electrons in the blob. The SSC spectrum exhibits a broad hump without strong spectral break, peaking around  $\langle \epsilon \rangle_{SSC} \approx (B'/B_{cr}) D \gamma_e^4 \approx \langle \epsilon \rangle_{sy} \gamma_e^2$ , where  $B'$  is the co-moving magnetic field,  $B_{cr} = 4.414 \cdot 10^{13}$  G, and  $D = (\Gamma [1 - \beta_\Gamma \cos \theta_{obs}])^{-1}$  is the Doppler factor associated with the bulk motion of the blob. Throughout this paper, all photon energies are described by the dimensionless quantity  $\epsilon = h\nu/(m_e c^2)$ .

If the blob is sufficiently far from the central engine of the AGN so that the accretion disk can be approximated as a point source of photons, its photon energy density (in the co-moving frame) is  $u'_D \approx L_D / (4\pi z^2 c \Gamma^2)$ , where  $L_D$  is the accretion disk luminosity, and  $z$  is the height of the blob above the accretion disk. The ECD spectrum can exhibit a strong spectral break, depending on the existence of a low-energy cutoff in the electron distribution function, and peaks at  $\langle \epsilon \rangle_{ECD} \approx \langle \epsilon \rangle_D (D/\Gamma) \gamma_e^2$ , where  $\langle \epsilon \rangle_D$  is the average photon energy of the accretion disk radiation (typically of order  $10^{-5}$  for geometrically thin, optically thick accretion disks around black holes of  $\sim 10^8 - 10^{10} M_\odot$ ).

Part of the accretion disk and the synchrotron radiation will be reprocessed by circumnuclear material in the broad line region and can re-enter the jet. Since this reprocessed radiation is nearly isotropic in the rest-frame of the AGN, it will be strongly blue-shifted

into the rest-frame of the relativistically moving plasma blob. Thus, assuming that a fraction  $a_{BLR}$  of the radiation is rescattered into the jet trajectory, we find for the energy density of rescattered accretion disk photons:  $u'_{ECC} \approx L_D a_{BLR} \Gamma^2 / (4\pi \langle r \rangle_{BLR}^2 c)$ , where  $\langle r \rangle_{BLR}$  is the average distance of the BLR material from the central black hole. The ECC photon spectrum peaks around  $\langle \epsilon \rangle_{ECC} \approx \langle \epsilon \rangle_D D \Gamma \gamma_e^2 \approx \langle \epsilon \rangle_{ECD} \Gamma^2$ .

For the synchrotron mirror mechanism, additional constraints due to light travel time effects need to be taken into account in order to estimate the reflected synchrotron photon energy density (for a detailed discussion see Böttcher & Dermer 1998), which is well approximated by  $u'_{RSy} \approx u'_{sy} 4 \Gamma^3 a_{BLR} (R'_B / \Delta r_{BLR}) (1 - 2 \Gamma R'_B / z)$ , where  $\Delta r_{BLR}$  is a measure of the geometrical thickness of the broad line region. Similar to the SSC spectrum, the RSy spectrum does not show a strong spectral break. It peaks around  $\langle \epsilon \rangle_{RSy} \approx (B' / B_{cr}) D \Gamma^2 \gamma_e^4 \approx \langle \epsilon \rangle_{SSC} \Gamma^2$ .

The energy density of the radiation field provided by IR emission from circumnuclear dust is  $u'_{IR} \sim 4 \Gamma^2 \xi_{IR} \sigma T_{dust}^4 / c$ , where  $\xi_{IR}$  is the fraction of the flux from the central source (accretion disc) reprocessed by the warm dust of temperature  $T_{dust}$ . Both  $\xi_{IR}$  and  $T_{dust}$  depend on the characteristic distance  $r_{IR}$  of the dust from the central source (Blăzejowski et al. 2000). The resulting Compton scattered radiation peaks around  $\langle \epsilon \rangle_{ECIR} \sim 3 k T_{dust} D \Gamma \gamma_e^2$ .

### 3. Spectral modeling of FSRQs and BL Lacs

The leptonic jet models described in the previous section have been used very successfully to model simultaneous broadband spectra of several FSRQs, LBLs, and HBLs. As more detailed spectral information has become available, the results of such broadband spectral modeling are now converging towards a rather consistent picture (e.g., Ghisellini et al. 1998, Kubo et al. 1998): The spectral sequence from HBLs to LBLs and on to FSRQs appears to be related to an increasing contribution of the external Comptonization mechanisms ECD and ECC to the  $\gamma$ -ray spectrum. While most FSRQs are successfully modelled with external Comptonization models (e. g., Dermer et al. 1997, Sambruna et al. 1997, Mukherjee et al. 1999, Hartman et al. 2001a), the broadband spectra of HBLs are consistent with pure SSC models (e. g., Mastichiadis & Kirk 1997, Pian et al. 1998, Petry et al. 2000). BL Lacertae, a LBL, appears to be intermediate between these two extremes, requiring an external Comptonization component to explain the EGRET spectrum (Madejski et al. 1999, Böttcher & Bloom 2000). As an example, Fig. 3 shows a fit to the simultaneous broadband spectrum of 3C 279 during the 1991 June flare state (Hartman et al. 1996, Hartman et al. 2001a).

A physical interpretation of this sequence in the framework of a unified jet model for blazars was given in Ghisellini et al. (1998). Assume that the average energy of electrons,  $\gamma_e$ , is determined by the balance of an energy-independent acceleration rate  $\dot{\gamma}_{acc}$  and radiative losses,  $\dot{\gamma}_{rad} \approx -(4/3) c \sigma_T (u' / m_e c^2) \gamma^2$ , where the target photon density  $u'$  is the sum of the sources intrinsic to the jet,  $u'_B + u'_{sy}$  plus external photon sources,  $u'_{ECD} + u'_{ECC} + u'_{RSy}$ . The average electron energy will then be  $\gamma_e \propto (\dot{\gamma}_{acc} / u')^{1/2}$ . If one assumes that the properties determining the acceleration rate of relativistic electrons do not vary significantly between different blazar subclasses, then an increasing energy density of the external radiation field will obviously lead to a stronger radiation component

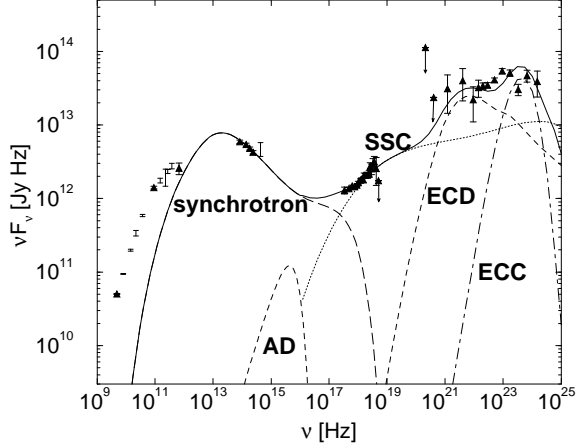


**Figure 3.** Fit to the simultaneous broadband spectrum of 3C 279 during the flare of 1991 June (Hartman et al. 1996). For model parameters see Hartman et al. (2001a).

due to external Comptonization, but also to a decreasing average electron energy  $\gamma_e$ , implying that the peak frequencies of both spectral components are displaced towards lower frequencies.

#### 4. Modeling of spectral variability of blazars

As described in the Introduction, HBLs exhibit rather consistent spectral variability patterns during flaring episodes, which have been very successfully reproduced by time-dependent model simulations in the framework of SSC-dominated jet models. In particular, the observed time lags between flares at different frequencies can be related to the magnetic field  $B$  and the Doppler boosting factor  $D$  through

$$t(\nu_1) - t(\nu_2) \propto B^{-3/2} D^{-1/2} \left( \nu_1^{-1/2} - \nu_2^{-1/2} \right) \quad (1)$$

(Takahashi et al. 1996). Also, the clockwise rotation of the spectral states of Mrk 421 and PKS 2155-304 has been modeled with a finite time scale of injection and/or acceleration of ultrarelativistic electrons along the jet — where, phenomenologically, the flare results primarily from an increasing high-energy cut-off  $\gamma_2$  of the injected electron distribution —, followed by radiative cooling, primarily due to synchrotron emission (e.g., Kirk et al. 1998, Georganopoulos & Marscher 1998a, Kataoka et al. 2000, Kusunose et al. 2000, Li & Kusunose 2000).

The modeling of spectral variability described above refers to the synchrotron component of HBLs which often peaks in the X-ray regime, where — at least during flares — useful spectral information is achievable within a few ksec of integration time. However, at  $\gamma$ -ray energies, such information generally requires integration times longer than the expected synchrotron cooling time scale. Thus, at present, such detailed short-term

variability models cannot be compared directly to  $\gamma$ -ray observations. However, a comparison of averaged broadband spectra over longer time scales may still provide useful model constraints. Comparing detailed spectral fits to weekly averaged broadband spectra of Mrk 501 over a period of 6 months, Petry et al. (2000) have found that TeV and hard X-ray high states on intermediate timescales are consistent with a hardening of the electron spectrum (decreasing spectral index) and an increasing number density of high-energy electrons, while the value of  $\gamma_2$  has only minor influence on the weekly averaged spectra. Fig. 4 shows the expected track of the time-averaged fluxes (on  $\sim$  weekly time scales) in the RXTE ASM and at  $> 1.5$  TeV in the case of a change of only one model parameter in a basic SSC model. The relatively large scatter of the observed correlation between the weekly averaged X-ray and the TeV  $\gamma$ -ray emission (see Figs. 6 and 7 of Petry et al. 2000) indicates that the long-term spectral variability of Mrk 501 might be associated with a change of more than one of the basic model parameters between high and low X-ray and  $\gamma$ -ray states.

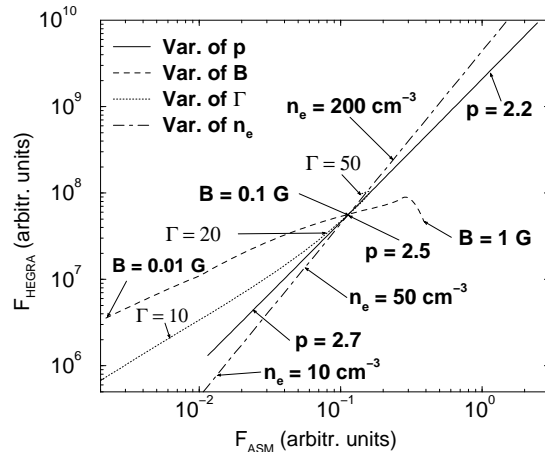


**Figure 4.** Expected correlation between the RXTE ASM and the HEGRA  $> 1.5$  TeV flux calculated from a time-averaged SSC model similar to the analytic model of Tavecchio et al. (1998) — from Petry et al. (2000).

While the rapid variability of HBLs can be rather well modelled and understood in the framework of SSC models, a similarly detailed and meaningful analysis of the rapid variability of quasars is until now hampered by (a) the lack of consistent variability patterns among different objects and even within the same object, and (b) the larger number of parameters entering the multi-component high-energy spectral calculations required to provide acceptable fits to FSRQ broadband spectra. In particular, in the framework of leptonic jet models, rapid variability will be influenced by (1) temporal variations of the seed photon fields for Comptonization (see, e.g., Böttcher & Dermer 1998 for a discussion of the isolated effect of such variability), (2) time-dependent electron acceleration and/or injection, and (3) time-dependent electron cooling. Given the limited time and frequency coverage available in simultaneous broadband observing campaigns

to date, it is virtually impossible to disentangle the isolated effects of these causes of variability on the basis of currently available data.

A promising first step towards understanding the rapid variability of quasars has recently been undertaken by Sikora et al. (2001), who have investigated a time-dependent shock-in-jet model with parameters appropriate to reproduce FSRQ-like broadband spectra. The basic idea of extracting physical information from observed variability patterns in quasars is that within a spectral region dominated by the contribution from only one radiation mechanism, time-lag features similar to the ones seen in the X-ray – UV – optical spectra in HBLs should result. From the fact that this is not consistent with the correlated X-ray /  $\gamma$ -ray variability of 3C 279, Sikora et al. (2001) conclude that the X-ray emission from this object is dominated by a different mechanism — most likely SSC — than the  $\gamma$ -rays, which might be dominated by Comptonization of external radiation. This agrees very well with the spectral modeling results of Hartman et al. (2001a).

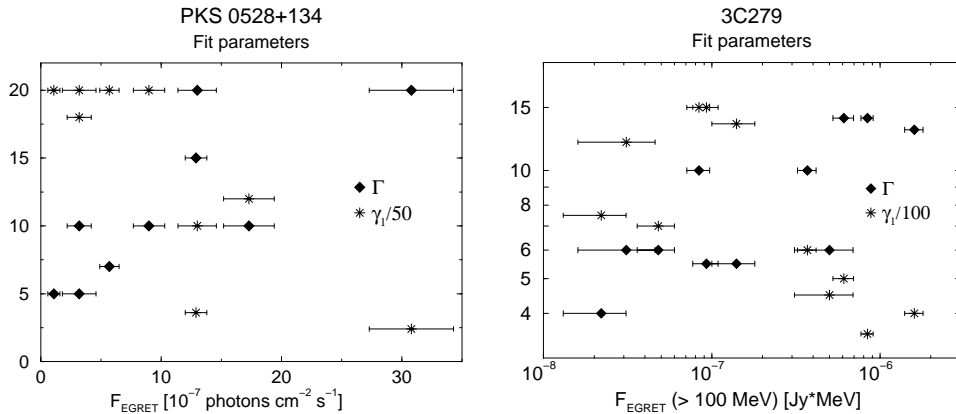


**Figure 5.** Model fit parameters  $\gamma_1$  (low-energy cut-off of the electron distribution) and  $\Gamma$  (bulk Lorentz factor) for PKS 0528+134 and 3C 279 during different  $\gamma$ -ray intensity states (Mukherjee et al. 1999, Hartman et al. 2001a).

In the case of quasars it is even more difficult to obtain time-dependent spectral information near the  $\gamma$ -ray peak, which is generally located in the GeV regime, only accessible to satellite-borne instruments. Even for the brightest quasar flares observed by EGRET, useful spectral information could only be extracted on time scales of a few days. However, during its  $\sim 9$  year lifetime EGRET has observed several  $\gamma$ -ray quasars multiple times in drastically different  $\gamma$ -ray intensity states, so that a meaningful broadband variability study of those objects can be done by comparing simultaneous broadband spectra in different EGRET observing periods. Such an analysis, accompanied with detailed spectral modeling of each individual simultaneous broadband spectrum, has been done for PKS 0528+134 (Mukherjee et al. 1999) and 3C 279 (Hartman et al. 2001a). In order to model the broadband spectra, as many model parameters as possible have been held fixed between different viewing periods. The long-term variability of those two objects could be reasonably well reproduced with a higher bulk Lorentz factor

and a lower low-energy cut-off  $\gamma_1$  of the electron distribution during higher  $\gamma$ -ray states. Fig. 5 illustrates these trends. They bear a striking similarity to the trend between different blazar sub-classes in the sense that a higher  $\gamma$ -ray luminosity indicates a stronger contribution from Comptonization of external radiation, accompanied by a lower value of  $\gamma_1$ . The analogy is mediated by the stronger  $\Gamma$ -dependence of the external Compton radiation component compared to the SSC component (Dermer 1995), leading to an increasing contribution from external-radiation Comptonization with increasing  $\Gamma$ .

However, it needs to be pointed out that due to the rather large number of parameters necessary to achieve acceptable broadband fits, other driving mechanisms for the long-term spectral variability of those two quasars (for example, a change of the magnetic-field configuration combined with other plausible parameter changes, which have not been investigated in Mukherjee et al. [1999] and Hartman et al. [2001a]) can not be ruled out at this point.

## 5. Challenges for future observations

In the previous sections, it has become clear that in particular the blazar sub-classes of FSRQs and LBLs still pose many unsolved questions as to the composition of their high-energy spectra and the dominant acceleration and cooling mechanisms for relativistic electrons in the jet. Two spectral regimes appear to be critical to better understand those mechanisms:

(1) More continuous frequency and time coverage of quasar spectral variability at optical – UV – soft X-ray frequencies would allow the identification of acceleration- and cooling-related variability patterns in the synchrotron component of FSRQs and LBLs. In particular, on the basis of a comparison of optical/UV and soft X-ray variability one would be able to pin down the transition between the emission from slow to fast cooling electrons and thus obtain accurate estimates of the magnetic fields and Doppler factors of quasar and LBL jets as well as additional size scale constraints. Dedicated monitoring observations with Chandra and XMM-Newton would be the ideal tool to achieve the X-ray aspect of this challenge.

(2) In the most successful spectral quasar and LBL models, one expects the transition between SSC-dominated and external-Compton-dominated emission in the hard X-ray / soft  $\gamma$ -ray regime, in which it is hard to achieve high-sensitivity observations with moderate spectral resolution. However, this would be required in order to confirm the predicted spectral hardening between the SSC and the external-Compton components. This transition should also have very characteristic imprints on the variability patterns, as pointed out by Sikora et al. (2001). Unfortunately, it seems unlikely that the upcoming INTEGRAL mission has sufficient sensitivity to allow spectral and variability studies of quasars and LBLs in the  $\sim 100$  keV – 10 MeV regime to place severe constraints on current models. Planned, more sensitive future missions, such as EXIST and the ACT, may be required to achieve those goals.

## References

Arbeiter, C., Pohl, M., & Schlickeiser, R., 2001, *A&A*, submitted.

Bednarek, W., 1998, *A&A*, 342, 69.

Blandford, R. D., & Levinson, A., 1995, *ApJ*, 441, 79.

Blażejowski, M., et al., 2000, *ApJ*, 545, 107.

Bloom, S. D., & Marscher, A. P., 1996, *ApJ*, 461, 657.

Böttcher, M., 1999, *ApJ*, 515, L21.

Böttcher, M., & Bloom, S. D., 2000, *AJ*, 119, 469.

Böttcher, M., & Dermer, C. D., 1998, *ApJ*, 501, L51.

Böttcher, M., Mause, H., & Schlickeiser, R., 1997, *A&A*, 324, 395.

Bradbury, S. M., et al., 1997, *A&A*, 320, L5.

Catanese, M., et al., 1998, *ApJ*, 501, 616.

Chadwick, P. M., et al., 1999, *ApJ*, 513, 161.

Dermer, C. D., 1995, *ApJ*, 446, L63.

Dermer, C. D., Schlickeiser, R., & Mastichiadis, A., 1992, *A&A*, 256, L27.

Dermer, C. D., & Schlickeiser, R., 1993, *ApJ*, 416, 458.

Dermer, C. D., Sturner, S. J., & Schlickeiser, R., 1997, *ApJS*, 109, 103.

Edelson, R., et al., 1995, *ApJ*, 438, 120.

Gaidos, J. A., et al., 1996, *Nature*, 383, 319.

Georganopoulos, M., & Marscher, A. P., 1998a, *ApJ*, 506, L11.

Georganopoulos, M., & Marscher, A. P., 1998b, *ApJ*, 506, 621.

Ghisellini, G., & Madau, P., 1996, *MNRAS*, 280, 67.

Ghisellini, G., et al., 1998, *MNRAS*, 301, 451.

Hartman, R. C., et al., 1996, *ApJ*, 461, 698.

Hartman, R. C., et al., 1999, *ApJS*, 123, 79.

Hartman, R. C., et al., 2001a, *ApJ*, 553, in press.

Hartman, R. C., et al., 2001b, *ApJ*, in press.

Kataoka, J., et al., 2000, *ApJ*, 528, 243.

Kirk, J. G., Rieger, F. M., & Mastichiadis, A., 1998, *A&A*, 333, 452.

Kubo, H., et al., 1998, *ApJ*, 504, 693.

Kusunose, M., Takahara, F., & Li, H., 2000, *ApJ*, 536, 299.

Li, H., & Kusunose, M., 2000, *ApJ*, 536, 729.

Madejski, G., et al., 1999, *ApJ*, 521, 145.

Mannheim, K., 1993, *A&A*, 269, 67.

Maraschi, L., Ghisellini, G., & Celotti, A., 1992, *ApJ*, 397, L5.

Marscher, A. P., & Gear, W. K., 1985, *ApJ*, 298, 114.

Mastichiadis, A., & Kirk, J. G., 1997, *A&A*, 320, 19.

Mücke, A., & Protheroe, R. J., 2001, *Astrop. Phys.*, 15, 121.

Mukherjee, R., et al., 1997, *ApJ*, 490, 116.

Mukherjee, R., et al., 1999, *ApJ*, 527, 132.

Petry, D., et al., 1996, *A&A*, 311, L13.

Petry, D., et al., 2000, *ApJ*, 536, 742.

Pian, E., et al., 1998, *ApJ*, *ApJ*, 492, L17.

Punch, M., et al., 1992, *Nature*, 358, 477.

Quinn, J., et al., 1996, *ApJ*, 456, L83.

Rachen, J., 1999, *AIP Conf. Proc.*, 515, 41.

Sambruna, R., et al., 1997, *ApJ*, 474, 639.

Schlickeiser, R., 1996, *Space Sci. Rev.*, 75, 299.

Sikora, M., Begelman, M. C., & Rees, M. J., 1994, *ApJ*, 421, 153.

Sikora, M., et al., 2001, *ApJ*, in press.

Takahashi, T., et al., 1996, *ApJ*, 470, L89.

Tavecchio, F., Maraschi, L., & Ghisellini, G., 1998, *ApJ*, 509, 608.

Urry, C. M., et al., 1997, *ApJ*, 486, 799.

von Montigny, C., et al., 1995, *ApJ*, 440, 525.

Wehrle, A., et al., 1998, *ApJ*, 497, 178.